Metal–Metal Interactions

Deutsche Ausgabe: DOI: 10.1002/ange.201505736
Internationale Ausgabe: DOI: 10.1002/anie.201505736

Direct X-Ray Scattering Evidence for Metal–Metal Interactions in Solution at the Molecular Level

Andrea Cebollada, Alba Vellé, Manuel Iglesias, Lauren B. Fullmer, Sara Goberna-Ferrón, May Nyman, and Pablo J. Sanz Miguel**

Abstract: *The study of the aggregation of small molecules in solution induced by metallophilic interactions has been traditionally performed by spectroscopic methods through identification of chemical changes in the system. Herein we demonstrate the use of SAXS (small-angle X-ray scattering) to identify structures in solution, taking advantage of the excellent scattering intensity of heavy metals which have undergone association by metallophilic interactions. An analysis of the close relationship between solid-state and solution arrangements of a dynamic $[Ag_2(bisNHC)_2]^{2+}$ (NHC = N-heterocyclic carbene) system, and how they are complementary to each other, is reported.*

The research field of metallophilic interactions has undergone significant development and has attracted intense interest over the last three decades.[1] An increasing number of examples have been reported in which the binding strength and nature of interconnected metal ions influence the structure and physical characteristics of the resulting materials. Metal–metal interactions, and in particular, argentophilic interactions,[2] are a keystone in numerous assemblies, including in host–guest systems,[2] nanoparticles,[3] and in conducting,[4] luminescent,[5] and/or framework materials.[6] Traditionally, metallophilic contacts exhibiting short metal–metal distances have been characterized in the solid-state by X-ray crystallographic studies. More importantly, the interactions in solution have been probed by spectroscopic methods (such as IR, Raman, UV/Vis, NMR, and ESR spectroscopies) and computational techniques have also been important in the study of such contacts.[7] Although small-angle X-ray scattering (SAXS) has been used extensively to probe the size, shape, and interactions of biomolecules,[8] prenucleation clusters,[9] discrete clusters,[10] and nanoparticles[11] in solution, metal–metal interactions have not been explored with this method. While the strong scattering between heavy metals is conducive to this technique, the small size of molecular species renders interpretation of data challenging. However, understanding the relationship between structure in solids and solution is of paramount importance in understanding natural phenomena and controlling synthetic processes. Herein we are able to distinguish between two conformers by SAXS, where the discrete state changes with solution conditions. This result is confirmed by the fact that the two conformers crystallize under different conditions.

Recently, we observed unsupported argentophilic interactions in solution and in the solid state for a dynamic cationic Ag complex, namely $[Ag_2(bisNHC)_2]^{2+}$ (NHC = N-heterocyclic carbene), which has the ability to act as an excellent host for silver ions and to aggregate in solution.[2g] We suspect that the strong donor properties of some ligands effectively alter the electronic properties of closed-shell metal ions, enhancing the metallophilic attractive forces between them. In this work, we carried out a parallel study of two $[Ag_2(bisNHC)_2]^{2+}$ ions employing methylenebis(*N*-2-methoxyethyl)imidazole-2-ylidene (bisMeOEtIm) as the ligand within the cation of **1** and methylenebis(*N*-2-butyl)imidazole-2-ylidene (bisBuIm) as the ligand within the cation of **2**. The behavior of $[Ag_2(bisMeOEtIm)_2](NO_3)_2$ (**1**) in solution[2g] is to a large extent analogous to that of **2** (see below). When dissolved, $[Ag_2(bisNHC)_2]^{2+}$ exists in two switchable conformations, denoted U and Z. The higher stability of isomer U is predicted by DFT calculations,[2g] and the equilibrium between both conformers is very sensitive to variations in the concentration, temperature, and/or the presence of additional Ag^+ ions.

An acetonitrile solvate of **1** was crystallized at −20 °C as $[Ag_2(bisMeOEtIm)_2](NO_3)_2{\cdot}CH_3CN$ (**1a**), which displays an open-book (U) conformation (see Figure S1 in the Supporting Information).[19] The dihedral (open-book) angle in **1a** (66.39(5)°) is slightly smaller to that of **1** (73.38(7)°), whereas the bonding environment of the Ag^+ cations is similar. An interesting feature is the lengthening of the intramolecular Ag–Ag bond in **1a** (Ag1–Ag2 3.6698(6) Å). This distance, which is greater than twice the van der Waals radius of silver ($2 \times 1.72 = 3.44$ Å), is even longer than that observed for the related cation–cation host–guest system $[Ag(CH_3CN)_2]^+ \subset [Ag_2(bisNHC)_2]^{2+}$ (3.6587(4) Å).[2g] Consequently, intramolecular Ag···Ag interactions within **1a** should be probably ruled out. Nevertheless, as shown in Figure 1, cations of **1a** associate in the solid state, stabilizing a rare example of a pair of cations[12] with an intermolecular Ag2–Ag2′ distance of 3.4786(6) Å. Although longer than 3.44 Å, this intermetallic separation seems to be enough to maintain relatively strong

[*] A. Cebollada,[+] A. Vellé, Dr. M. Iglesias, Dr. P. J. Sanz Miguel
Departamento de Química Inorgánica
Instituto de Síntesis Química y Catálisis Homogénea (ISQCH)
Universidad de Zaragoza-CSIC, 50009 Zaragoza (Spain)
E-mail: pablo.sanz@unizar.es
L. B. Fullmer, Dr. S. Goberna-Ferrón, Dr. M. Nyman
Center for Sustainable Materials Chemistry
Department of Chemistry, Oregon State University
Corvallis, OR 97331-4003 (USA)
E-mail: May.Nyman@oregonstate.edu
[+] Visiting scholar at Oregon State University.

Supporting information (including structural details, NMR measurements, SAXS data, X-ray diffraction details, and ESI-MS data) and ORCID(s) from the author(s) for this article are available on the WWW under http://dx.doi.org/10.1002/anie.201505736.

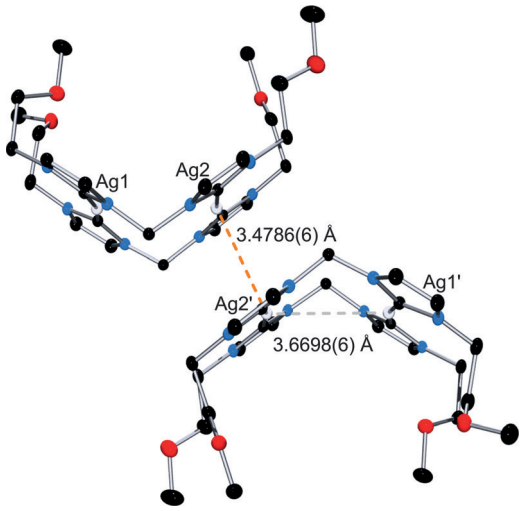

Figure 1. Ag···Ag distances (denoted by dashed lines) between cations of **1a**. Ag atom color = light gray.

argentophilic interactions. We assume that Ag···Ag interactions might exceed the limits of the van der Waals radii if strong donor ligands are involved.[13] Interestingly, a search in the CCDC database (June 2015) revealed a considerable number of examples having Ag–Ag distances greater than 3.44 Å (Figure S2). A similar tendency should be expected for other closed-shell metals.

The butyl-functionalized derivative of this system was synthesized in an analogous manner to **1**. $[Ag_2(bisBuIm)_2](NO_3)_2$ (**2**) could be independently isolated in the solid state in both conformations: U-$[Ag_2(bisBuIm)_2](NO_3)_2$ (**2a**)[14] and Z-$[Ag_2(bisBuIm)_2](NO_3)_2$ (**2b**). Crystallization of **2a** was performed at room temperature, whereas **2b** was isolated as a polycrystalline aggregate at 40 °C. In solution, both conformers rapidly interconvert. X-ray diffraction measurements at different temperatures (100–298 K) show that the geometry of the $[Ag_2(bisNHC)_2]^{2+}$ ions are not significantly affected by temperature.[15]

The geometry of the U conformer **2a** (Figure 2a) is almost identical to that of the cation of **1**, except for the side arms.[19] For **2a**, the dihedral ("open-book") angle is 73.38(5)° and the separation between the silver atoms (Ag1–Ag2) has a distance of 3.4431(3) Å, whereas for **1** these values

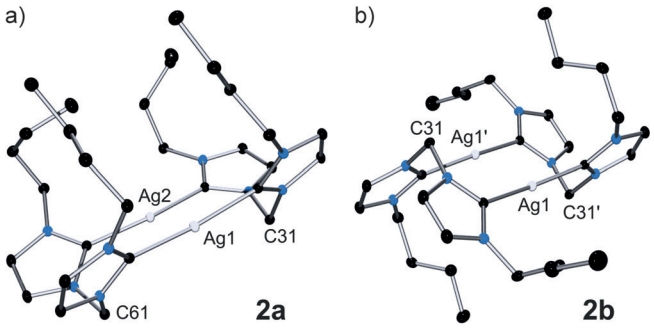

Figure 2. The X-ray structures of a) the U conformer (**2a**) and b) the Z conformer (**2b**) of **2**. Ag–Ag distances [Å]: 3.4431(3) (**2a**), 3.2308(11) (**2b**). Symmetry operation (**2b**): 1−*x*, −y, 1−*z*.

measured 73.38(7)° and 3.4512(5) Å. A remarkable difference is found in the crystal packing: cations of **2a** follow a similar tendency to stabilize pairs of cations as evident in **1a**. In this case, the intermolecular Ag1–Ag1′ distance measures 3.5020(4) Å.

On the other hand, the molecular arrangement of the centrosymmetric Z conformer **2b** (Figure 2b) differs structurally in the relative positioning of the ligands.[19] The bridged imidazole rings of an NHC ligand and the cross-linked imidazole rings of the symmetry-related ligand form roughly right angles (89.77(9)°). In this case, intramolecular Ag···Ag interactions are shorter (Ag1–Ag1′ 3.2308(11) Å) than in complexes **2a** and **1**, although the interaction distance seems not to have a critical influence on the bonding environment of silver (Ag1–C22 2.094(2) Å; Ag1–C12 2.094(2) Å; C22-Ag1-C12 167.85(8)°). It should be mentioned here that the mutual disposition of the NHC ligands in **2b** avoids further metal–metal interactions between the silver ions, as the methylene bridge and the side arms hinder this possibility.

Compound **2** was characterized in solution (Figures S3–S6), and its behavior thoroughly evaluated by ^{1}H NMR spectroscopy (concentration, temperature, addition of Ag^+). NMR experiments revealed that compound **2** behaved analogously to **1** (Figures S7–S10), despite the lower solubility of **2**. Thus, a dynamic behavior (U⇌Z) influenced by temperature and argentophilic interactions was observed (Figures S8–S10). This is not surprising considering the structural similarity between both compounds. An interesting aspect here is the effect of intermolecular interactions over the U/Z conversion rate. Increasing the concentration of compound **2** implies the presence of a higher number of molecules in close proximity, and therefore leading to intermolecular argentophilicity, as demonstrated by ^{1}H NMR spectroscopy (Figure S10). With the formation of cation–cation aggregates in solution, a corresponding weakening of the intramolecular Ag···Ag attraction occurs. This results in the lengthening of the intramolecular contacts and the subsequent shortening of the intermolecular Ag–Ag distances (a conceptual illustration thereof is shown in Figure 1), and therefore in a smaller energy barrier for the U⇌Z equilibrium (faster exchange, as confirmed by ^{1}H NMR spectroscopy). This is consequent with the fact that in the ^{1}H NMR spectrum the H5 signals (see Figure 3 for NMR labelling of the system) for protons on the imidazole rings shift downfield in highly concentrated samples as a result of increasing Ag···Ag interactions, whereas at higher temperatures this shift is not observed and only a gradual sharping of the proton signals attributable to the CH_2 bridge takes place.

SAXS studies were carried out for the ether derivative **1** because of the poorer solubility of **2**. Nevertheless, an analogous behavior can be inferred for **2**. We analyzed different variables, specifically concentration changes, addition of $AgNO_3$, and of nitrate anions (as the tetrabutylammonium salt). We utilized two different approximations to corroborate the radius of gyration R_g (a shape independent measure of size from the summation of scattering vectors from the center of mass of a particle): 1) the Guinier approximation[16] and 2) the pair distance distribution func-

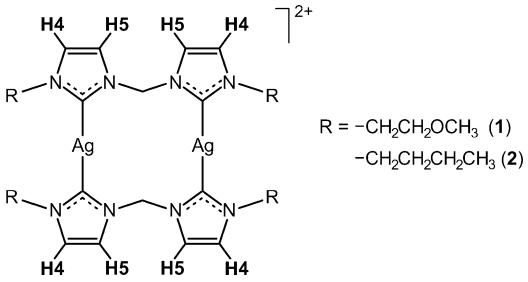

Figure 3. Atom labelling of cations of **1** and **2** for NMR experiments.

Table 1: Radius of gyration (R_g) from simulated and experimental scattering data for **1** in CH_3CN.

Compound	R_g (Guinier) [Å]	R_g (PDDF) [Å]
Simulated from solid-state structure:		
1a (U conformation)	3.2	3.4
1a (dimer of U conformation)	4.6	4.8
2a (U conformation)	2.9	3.1
2b (Z conformation)	2.9	3.0
Experimental:		
1 (100 mM)	3.1	3.0
1 (50 mM)	3.5	3.4
1 (25 mM)	3.7	3.5
1 (10 mM)	3.9	3.7

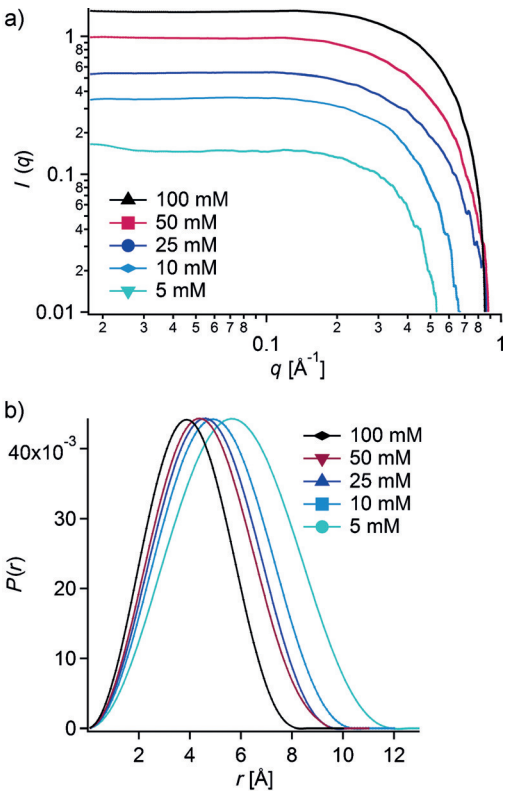

Figure 4. a) Log q–log $I(q)$ X-ray scattering curves of **1** in acetonitrile at different concentrations and b) the corresponding intensity-normalized PDDFs from Fourier transform of these scattering curves.

tion (PDDF; the Fourier transform method of Moore).[17] Values obtained in both cases are similar, suggesting that despite the relatively small size of the species, robust and informative data can be obtained. In order to check the validity of our system to be studied by SAXS, scattering data was simulated[18] (Table 1) from solid-state structures. Theoretical and experimental R_g values were obtained in the same range, and the simulated and experimental scattering curves display similar profiles (Figure S11). Thus, these simulations evidence the reliability of the experimental data, even though these scattering species are considerably smaller than those commonly analyzed with SAXS.

Upon dissolution of **1** in acetonitrile, two major interrelated phenomena take place, namely, U/Z conversion and metallophilic interactions. A snapshot at moderate temperatures (close to room temperature), would in principle reveal most of the molecules to be present in their U form because of its higher stability compared to the Z isomer. As outlined above, the U/Z conformational change is promoted by intermolecular interactions and increasing temperatures. A percentage increase of the Z conformer would be expected in solution at higher concentrations (or temperatures). In fact, crystallization of the Z-shaped cation of **2b** at 40 °C supports this premise. Considering that a higher proportion of the Z isomer "inhibits" the formation of intermolecular argentophilic interactions, a smaller average scattering species should be expected for higher concentration samples. In addition, crystallographic intramolecular Ag···Ag separation exhibited by the Z rotamers is shorter than that in the U conformer (3.4431(3) Å (**2a**); 3.2308(11) Å (**2b**)), as shown in Figure 2. This too can contribute to both a smaller apparent scattering species (since most of the scattering comes from Ag···Ag interactions) and fewer intermolecular Ag···Ag interactions. Indeed, experimental SAXS data show a clear dependence between scattering species size (R_g) and concentration, with R_g values decreasing with increasing concentrations (Table 1). We attribute this to association of U conformers into dimers at lower concentration. This shows rare direct evidence by SAXS of argentophilic interactions in a molecular system. The PDDFs (Figure 4b) also show the increasing radius of approximately spherical scattering species with decreasing concentration, reflecting a higher portion of the U conformer that can readily dimerize through Ag···Ag interactions (as shown in Figure 1). However, the Gaussian single peak shape of the PDDF does not provide much information about the predominant geometry of the scattering species: this information we extract by shielding interactions with added electrolytes (see below).

The second SAXS study focuses on the addition of Ag^+ ions ($AgNO_3$) to a 50 mM solution of **1**. Before discussing the obtained results, it is worth mentioning that an aggregation tendency is observed in the SAXS scattering curve for an acetonitrile solution containing only silver nitrate, evident by a modest amount of X-ray scattering above background solvent scattering (Figure 5a). This provides additional SAXS evidence for argentophilicity in solution. These interactions between "free" silver atoms cannot be ignored, especially for high quantities of silver added.

As SAXS studies are related to the size of the particles, interpretation of experimental data presents here several

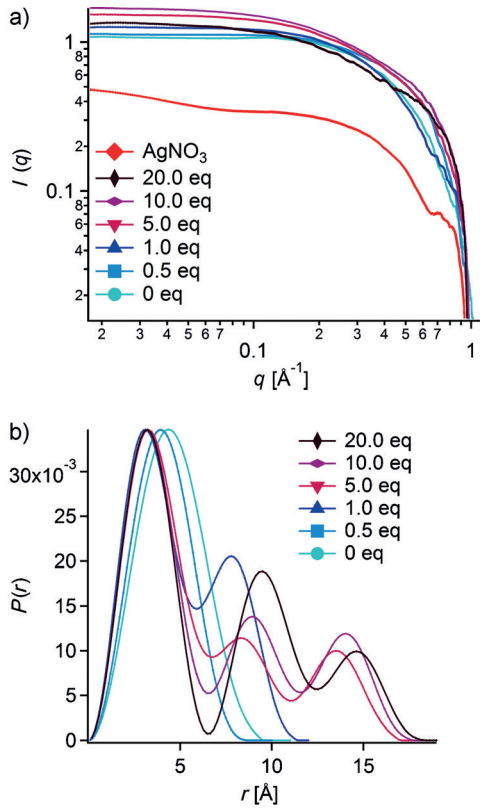

Figure 5. a) Log q–log $I(q)$ X-ray scattering curves of **1** (50 mM) dissolved in acetonitrile with different concentrations of $AgNO_3$, including a curve of $AgNO_3$ alone (50 mM), and b) the corresponding intensity-normalized PDDF spectra.

difficulties because of the existence of many different SAXS-detected phenomena in solution, for instance: 1) interactions between $[Ag_2(bisNHC)_2]^{2+}$ dimers; 2) interactions between free silver ions; 3) interactions involving dimers and free silver cations, including formation of host–guest systems $[Ag^I \subset Ag_2(bisNHC)_2]^{3+}$;[2g] 4) the influence of the counterions added with the silver (see below) in the system. Several models for the association between the dimers and the silver cations are shown (Figures S12 and S13). The last three cases will gain importance with the addition of considerable amounts of silver nitrate. The sum of all these factors generates scattering curves of high complexity. PDDF analysis suggests the formation of more complicated geometries after addition of $AgNO_3$, which cannot be easily interpreted (Figure 5).

The Guinier approximation shows an analogous tendency to the one observed in the concentration study: R_g values decrease with the addition of silver nitrate (Table S4). This is also evidenced by the minimal increase in scattering intensity in the Guinier region ($q < 0.1$ Å^{-1}) with added silver. The greatest contribution to scattering intensity in this region is the radius of scattering species (r^6 dependency). Therefore, if large species (silver nanoparticles for example) were forming, we would see a significant increase in scattering intensity. The slight increase in scattering intensity is related to more abundant interactions between the electron-dense silver ions: scattering intensity has a Z^2 dependency where Z = atomic number. The presence of silver ions increases the number of intermolecular argentophilic interactions, and therefore isomerization becomes more facile. These intermolecular interactions also lead to downfield shifts of the resonance signals for the H5 protons in the ^{1}H NMR spectra, as well as faster U/Z conversion, which is also evidenced in the sharpening of the resonance attributable to the CH_2 bridge (Figure S10).

With the aim of evaluating the influence of the nitrate counterions necessarily introduced with Ag^I and the shielding effects of electrolytes on the argentophilic interactions, tetrabutylammonium nitrate $NBu_4(NO_3)$ was added to acetonitrile solutions of **1**. Monitoring of the process by ^{1}H NMR spectroscopy (Figure 6) reveals: i) a substantial shift toward low field of the imidazole H5 signal (0.7 ppm), a clear indicator of the presence of intermolecular argentophilicity,

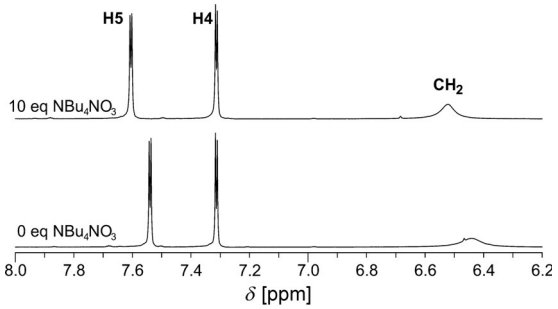

Figure 6. Low-field sections of ^{1}H NMR spectra (CD_3CN, 27 mM) of **1**, and after addition of 10 equiv of NBu_4NO_3.

and ii) that the resonance signal attributable to the methylene bridge does not become considerably sharper (even after addition of 10 equivalents of $NBu_4(NO_3)$). In the corresponding scattering data, we observe a distinct inflection point at circa 0.7 Å^{-1} with addition of $NBu_4(NO_3)$, often indicative of a dimeric species. Indeed, the PDDF (Figure 7b) analysis does show increasing intensity of a second peak with increasing $NBu_4(NO_3)$ concentration, which is a typical PDDF profile of a dimer such as **1a**. The PDDF from the Fourier transform of the simulated scattering curve of **1a** similarly shows this dimeric species (Figure S14). These data provide intriguing evidence that the U conformer of **1**, namely **1a**, which was isolated in the solid state, is likely the dominant isomer in solution when U to Z isomerization is suppressed.

In summary, here we present the first SAXS evidence of argentophilic interactions in solution at the molecular level involving, namely, $[Ag_2(bisNHC)_2]^{2+}$ ions and Ag^+ ions ($AgNO_3$). These results reflect the interacting situations observed in different solid-state arrangements of compounds **1** and **2**. Moreover, we postulate that if strong donor (NHC) ligands are involved, Ag···Ag interactions (or with other closed-shell metal ions) may be greater in length than the limits set by the van der Waals radii (Ag–Ag 3.44 Å). Our results show the clear influence of argentophilicity over the behavior of the $[Ag_2(bisNHC)_2]^{2+}$ system in solution. More broadly, this study shows the close relationship between ion interactions observed in solid-state structures and those observed in solution.

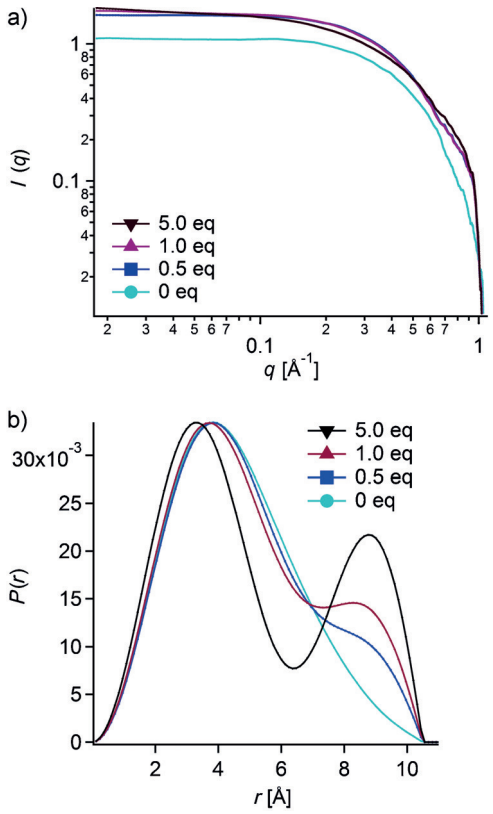

Figure 7. a) Log q–log $I(q)$ X-ray scattering curves of **1** (50 mM) dissolved in acetonitrile with different concentrations of $NBu_4(NO_3)$ and b) the corresponding intensity-normalized PDDF spectra.

Acknowledgements

We gratefully acknowledge financial support from the National Science Foundation (grant CHE-1102637), from the Center for Sustainable Materials Chemistry (L.B.F., S.G.F., and M.N.), and the Spanish Ministerio de Economía y Competitividad ("Ramón y Cajal" program (P.J.S.M.) and CTQ2011-27593).

Keywords: carbene ligands · metal–metal interactions · NMR spectroscopy · silver · small-angle X-ray scattering

How to cite: *Angew. Chem. Int. Ed.* **2015**, *54*, 12762–12766
Angew. Chem. **2015**, *127*, 12953–12957

[1] a) M. Jansen, *Angew. Chem. Int. Ed. Engl.* **1987**, *26*, 1098–1110; *Angew. Chem.* **1987**, *99*, 1136–1149; b) P. Pyykkö, *Chem. Rev.* **1997**, *97*, 597–636; c) H. Schmidbaur, *Gold Bull.* **2000**, *33*, 3–10; d) H. Schmidbaur, *Nature* **2001**, *413*, 31–33.

[2] a) T. Osuga, T. Murase, M. Fujita, *Angew. Chem. Int. Ed.* **2012**, *51*, 12199–12201; *Angew. Chem.* **2012**, *124*, 12365–12367; b) Y. Kohyama, T. Murase, M. Fujita, *Angew. Chem. Int. Ed.* **2014**, *53*, 11510–11513; *Angew. Chem.* **2014**, *126*, 11694–11697; c) T. Sawada, A. Matsumoto, M. Fujita, *Angew. Chem. Int. Ed.* **2014**, *53*, 7228–7232; *Angew. Chem.* **2014**, *126*, 7356–7360; d) A. Rit, T. Pape, F. E. Hahn, *J. Am. Chem. Soc.* **2010**, *132*, 4572–4573; e) X.-P. Zhou, Y. Wu, D. Li, *J. Am. Chem. Soc.* **2013**, *135*, 16062–16065; f) C.-Y. Gao, L. Zhao, M.-X. Wang, *J. Am. Chem. Soc.* **2012**, *134*, 824–827; g) A. Vellé, A. Cebollada, M. Iglesias, P. J. Sanz Miguel, *Inorg. Chem.* **2014**, *53*, 10654–10659.

[3] See, for example: a) A. Desireddy, B. E. Conn, J. Guo, B. Yoon, R. N. Barnett, B. M. Monahan, K. Kirschbaum, W. P. Griffith, R. L. Whetten, U. Landman, T. P. Bigioni, *Nature* **2013**, *501*, 399–402; b) X. He, X.-B. Xu, X. Wanga, L. Zhao, *Chem. Commun.* **2013**, *49*, 7153–7155; c) Y. Yao, K. Jie, Y. Zhou, M. Xue, *Chem. Commun.* **2014**, *50*, 5072–5074.

[4] a) K. M. Hutchins, T. P. Rupasinghe, L. R. Ditzler, D. C. Swenson, J. R. G. Sander, J. Baltrusaitis, A. V. Tivanski, L. R. MacGillivray, *J. Am. Chem. Soc.* **2014**, *136*, 6778–6781; b) S. L. Zheng, J. P. Zhang, W. T. Wong, X. M. Chen, *J. Am. Chem. Soc.* **2003**, *125*, 6882–6883.

[5] a) Y. Morishima, D. J. Young, K. Fujisawa, *Dalton Trans.* **2014**, *43*, 15915–15928; b) J. Zheng, Y.-D. Yu, F.-F. Liu, B.-Y. Liu, G. Wei, X.-C. Huang, *Chem. Commun.* **2014**, *50*, 9000–9002; c) A. A. Mohamed, A. Burini, J. P. Fackler, *J. Am. Chem. Soc.* **2005**, *127*, 5012–5013.

[6] a) W. Cai, A. Katrusiak, *Nat. Commun.* **2014**, *5*, 4337; b) M. A. Sinnwell, J. Baltrusaitis, L. R. MacGillivray, *Cryst. Growth Des.* **2015**, *15*, 538–541; c) Q. Chu, D. C. Swenson, L. R. MacGillivray, *Angew. Chem. Int. Ed.* **2005**, *44*, 3569–3572; *Angew. Chem.* **2005**, *117*, 3635–3638; d) T. Osuga, T. Murase, M. Hoshino, M. Fujita, *Angew. Chem. Int. Ed.* **2014**, *53*, 11186–11189; *Angew. Chem.* **2014**, *126*, 11368–11371; e) C.-Y. Gao, L. Zhao, M.-X. Wang, *J. Am. Chem. Soc.* **2011**, *133*, 8448–8451.

[7] For a recent review, see: H. Schmidbaur, A. Schier, *Angew. Chem. Int. Ed.* **2015**, *54*, 746–784; *Angew. Chem.* **2015**, *127*, 756–797 and references therein.

[8] C. D. Putnam, M. Hammel, G. L. Hura, J. A. Tainer, *Q. Rev. Biophys.* **2007**, *40*, 191–285.

[9] a) R. E. Ruther, B. M. Baker, J.-H. Son, W. H. Casey, M. Nyman, *Inorg. Chem.* **2014**, *53*, 4234–4242; b) D. Gebauer, H. Cölfen, *Nano Today* **2011**, *6*, 564–584.

[10] a) O. Sadeghi, L. N. Zakharov, M. Nyman, *Science* **2015**, *347*, 1359–1362; b) Y. Hou, L. N. Zakharov, M. Nyman, *J. Am. Chem. Soc.* **2013**, *135*, 16651–16657.

[11] a) H. Borchert, E. V. Shevchenko, A. Robert, I. Mekis, A. Kornowski, G. Grübel, H. Weller, *Langmuir* **2005**, *21*, 1931–1936; b) J. Polte, T. T. Ahner, F. Delissen, S. Sokolov, F. Emmerling, A. F. Thünemann, R. Kraehnert, *J. Am. Chem. Soc.* **2010**, *132*, 1296–1301.

[12] W. Gamrad, A. Dreier, R. Goddard, K.-R. Pörschke, *Angew. Chem. Int. Ed.* **2015**, *54*, 4482–4487; *Angew. Chem.* **2015**, *127*, 4564–4569 and references therein.

[13] S. Johannsen, N. Megger, N. Böhme, R. K. O. Sigel, J. Müller, *Nat. Chem.* **2010**, *2*, 229–234.

[14] For a hexafluorophosphate salt of **2a**, see: C. A. Quezada, J. C. Garrison, M. J. Panzner, C. A. Tessier, W. J. Youngs, *Organometallics* **2004**, *23*, 4846–4848.

[15] M. Kriechbaum, J. Hölbling, H.-G. Stammler, M. List, R. J. F. Berger, U. Monkowius, *Organometallics* **2013**, *32*, 2876–2884.

[16] A. Guinier, G. Fournet, *Small-Angle Scattering of X-Rays*, Wiley, New York, **1955**.

[17] B. Moore, *J. Appl. Crystallogr.* **1980**, *13*, 168–175.

[18] R. T. Zhang, P. Thiyagarajan, D. M. Tiede, *J. Appl. Crystallogr.* **2000**, *33*, 565–568.

[19] CCDC 1406442 (**1a**), 1406443 (**2a**), and 1406444 (**2b**) contain the supplementary crystallographic data for this paper. These data can be obtained free of charge from The Cambridge Crystallographic Data Centre.

Received: June 22, 2015
Revised: July 20, 2015
Published online: September 1, 2015

